Optical and Biodynamic Evaluation of the Helmet Integrated Display Sight System (HIDSS) for the RAH-66 Comanche Development and Validation Program Phase

By

Thomas H. Harding
Howard H. Beasley
John S. Martin

UES, Inc.

and
Clarence E. Rash
William E. McLean
John C. Mora

Aircrew Health and Performance Division

and
B. Joseph McEntire

Aircrew Protection Division

19980505 099

DTIC QUALITY INSPECTED

March 1998

U.S. Army Aeromedical Research Laboratory
Fort Rucker, Alabama 36362-0577

REPORT DOCUMENTATION PAGE

Form Approved
OMB No. 0704-0188

1a. REPORT SECURITY CLASSIFICATION Unclassified	1b. RESTRICTIVE MARKINGS

2a. SECURITY CLASSIFICATION AUTHORITY

2b. DECLASSIFICATION / DOWNGRADING SCHEDULE

3. DISTRIBUTION / AVAILABILITY OF REPORT
Approved for public release, distribution unlimited

4. PERFORMING ORGANIZATION REPORT NUMBER(S)
USAARL Report No. 98-22

5. MONITORING ORGANIZATION REPORT NUMBER(S)

6a. NAME OF PERFORMING ORGANIZATION U.S. Army Aeromedical Research Laboratory	6b. OFFICE SYMBOL (If applicable) MCMR-UAD	7a. NAME OF MONITORING ORGANIZATION U.S. Army Medical Research and Materiel Command

6c. ADDRESS (City, State, and ZIP Code)
P.O. Box 620577
Fort Rucker, AL 36362-0577

7b. ADDRESS (City, State, and ZIP Code)
Fort Detrick
Frederick, MD 21702-5012

8a. NAME OF FUNDING / SPONSORING ORGANIZATION	8b. OFFICE SYMBOL (If applicable)	9. PROCUREMENT INSTRUMENT IDENTIFICATION NUMBER

8c. ADDRESS (City, State, and ZIP Code)

10. SOURCE OF FUNDING NUMBERS

PROGRAM ELEMENT NO.	PROJECT NO.	TASK NO.	WORK UNIT ACCESSION NO.
62787A	30162787A879	PB	178

11. TITLE (Include Security Classification)
(U) Optical and biodynamic evaluation of the Helmet Integrated Display Sight System (HIDSS) for the RAH-66 Comanche, development and validation program phase

12. PERSONAL AUTHOR(S)
TH Harding, JS Martin, HH Beasley, CE Rash, WE McLean, JC Mora, & BJ McEntire

13a. TYPE OF REPORT Final	13b. TIME COVERED FROM TO	14. DATE OF REPORT (Year, Month, Day) 1998 March	15. PAGE COUNT 39

16. SUPPLEMENTAL NOTATION

17. COSATI CODES

FIELD	GROUP	SUB-GROUP
01	03	
09	05	

18. SUBJECT TERMS (Continue on reverse if necessary and identify by block number)
Comanche helmet-mounted display (HMD), Helmet Integrated Display Sight System (HIDSS), and optical testing

19. ABSTRACT (Continue on reverse if necessary and identify by block number)
The Development and Validation phase Helmet Integrated Display Sight System (HIDSS) for the RAH-66 Comanche was evaluated. The HIDSS consists of an integated helmet, a helmet-mounted display consisting of a right and a left multifunction display, a helmet tracking system, a boresight reticle unit, and the associated electronics. The evaluation consisted of biodynamic, optical, and visual performance measures. Measurements show that the HIDSS fails to provide acceptable weight and center of mass performance. At a value of 2.62 kg, the head supported weight exceeds the maximum allowable value. Image quality was acceptable except for the areas of contrast ratio (shades of gray), luminance uniformity, and modulation transfer function. Additional human factors engineering concerns surfaced during the evaluation. These included restrictions on pilot head movements due to cathode ray tube size and location, extraneous reflections, single visor configuration, and interpupillary distance extreme adjustment effect on monocular operation.

20. DISTRIBUTION / AVAILABILITY OF ABSTRACT ☐ UNCLASSIFIED/UNLIMITED ☒ SAME AS RPT. ☐ DTIC USERS	21. ABSTRACT SECURITY CLASSIFICATION Unclassified

22a. NAME OF RESPONSIBLE INDIVIDUAL Chief, Science Support Center	22b. TELEPHONE (Include Area Code) (334) 255-6907	22c. OFFICE SYMBOL MCMR-UAX-SI

DD Form 1473, JUN 86   Previous editions are obsolete.   SECURITY CLASSIFICATION OF THIS PAGE

Table of contents

List of figures

Table of contents (continued)

List of figures (continued)

List of tables

Introduction

The RAH-66 Comanche is the Army's next generation reconnaissance/attack rotary-wing aircraft. The Comanche Mission Equipment Package (MEP) includes a helmet mounted display designated as the Helmet Integrated Display Sight System (HIDSS). The Development and Validation Program (DVP) phase HIDSS consists of an integrated helmet, a helmet mounted display (HMD) consisting of a right and a left display channel, a helmet tracking source (HTS), a boresight reticle unit (BRU), and the associated electronics (e.g., enhanced display electronics unit [EDEU] and display control panel). Imagery acquired by nose-mounted forward-looking infrared (FLIR) or television sensors is reproduced on miniature displays and then optically relayed to the aviator's eyes. The HTS allows the nose mounted sensors to be slaved to the aviator's head movements. The BRU provides the capability to align the HTS to the straight ahead direction. The display control panel provides for display adjustments, e.g., brightness and contrast. The HIDSS is required to operate biocularly/binocularly with monocular capability. The HIDSS presents a 30°(V) X 52°(H) field-of-view (FOV) with a minimum 17° overlap. Exit pupil size is to be 15 mm on axis and 13 mm off axis. A design goal for minimum eye clearance is 22 mm. Kaiser Electronics, San Jose, California, is the manufacturer of the HIDSS evaluated herein. Gentex Corporation, Carbondale, Pennsylvania, manufactures the helmet shell and visor.

The Kaiser Electronics HIDSS

The Kaiser Electronics version of the HIDSS has a biocular/binocular integrated helmet and an HMD system. It consists of an aircraft retained unit (ARU) and a pilot retained unit (PRU) (Figure 1). The ARU is a front piece consisting of two miniature 1-inch diameter cathode ray tubes (CRTs) and two optical relays attached to a mounting bracket (Figure 2). The final elements of the optical relays are beamsplitters, referred to as combiners. The PRU is the basic helmet with a single-visor assembly. The Kaiser Electronics HIDSS uses two 35° monoculars which provide the required FOV. The system provides adjustments for interpupillary distance (IPD) and vertical adjustment position. Rubber baffles have been installed on the back sides of the combiners to reduce reflections.

Figure 1. The Kaiser Electronics HIDSS.

Figure 2. The relay optics with combiner.

Biodynamic characteristics

Head supported weight (mass)

Test equipment. Sartorius model LC12001P digital scale.

Test procedure. The Comanche HIDSS was placed on the scale and the mass was recorded. The HIDSS was removed and dummy representative communication and CRT cables were individually placed on the scale and their mass recorded. The HIDSS head supported mass was calculated by subtracting the dummy cables' mass from the HIDSS mass.

Results. The results of the mass measurements are provided in Table 1.

Table 1.
HIDSS head supported mass.

Component	Mass (gm)
Total HIDSS	3041.2
Dummy communication cord	21.0
Dummy CRT cable & connector	401.1
Head supported mass (calculated)	2619.1

Impact. The impact of the measured head supported mass value is a function of system center of mass. See discussion in the Center of mass section.

Center of mass (CM)

Test equipment. Space Electronics KSR 330 mass properties machine. The test fixture used for positioning the HIDSS was the U.S. Army Aeromedical Research Laboratory (USAARL) medium size (50th percentile) male headform.

Test procedure. The HIDSS was fitted onto the test headform and the optical system's adjustments for eye height, eye relief, and IPD adjusted for the headform's eye position. During CM measuring, the helmeted headform was positioned orthogonally in three orientations: XY, XZ, and YZ. To reduce operator error in HIDSS positioning, a minimum of three measurements were made in each headform orientation with the HIDSS being removed and repositioned between measurements. These results for each axis were averaged to obtain the reported result. During the headform tare process, the dummy cables (communication and CRT) were positioned in approximately the same location the HIDSS cables occupied during the measurements. This results in reducing the actual cable influence on the measured CM positions.

Results. The results of the center of mass measurements are provided in Table 2.

Table 2.
HIDSS center of mass.

Comanche HIDSS	x-axis	y-axis	z-axis
millimeters	34.02	3.38	48.41
inches	1.34	0.13	1.90

Impact. The amount of head supported mass and its CM location can affect many physiological parameters during normal operations and emergency situations. These physiological parameters, as a minimum, include transmitted neck loads, fatigue onset, biodynamic response changes, system comfort, and user acceptability.

The head supported mass and x- and z- axes relationships are illustrated in Figures 3 and 4 with the respective requirements. Figure 3 shows the measured mass and z-axis center of mass location to lie outside the accepted injury risk area of the constant moment curve (McEntire and Shanahan, 1996). If airbag restraint systems are used in the cockpit, these values are acceptable. Interpretation of this data point indicates the RAH-66 aircrew will be exposed to greater risk of sustaining a severe neck injury during helicopter mishaps than other Army aircrew.

Figure 4 shows the measured mass and z-axis CM location to lie also outside the acceptable region. This constant moment curve is based on significant changes in biodynamic response when exposed to helicopter vibration environments. The effects of prolonged or repeated exposures to these conditions are currently unknown, but it is possible that chronic pain and degenerative disorders may develop.

The effect of HIDSS mass coupled with CM location on system stability, fatigue, comfort and user acceptance are not addressed.

Optical characteristics

An optical test bench was used throughout to properly hold, align and actively measure the video response characteristics from the HIDSS. Optical alignment was achieved by affixing the ARU to the USAARL fabricated holder with precision rotation (resolution: ± 0.5 arc second) and linear X and Y positioners (resolution: ± 0.25 micron). See Figure 5 for a photograph of the experimental setup. For many of our physical measurements, we found it easier to mount only one optical/CRT channel to the rotating stage. Optical alignment was achieved by producing a centering video pattern consisting of a crosshair which extended to the far periphery of the

3

Head Worn Mass Criteria for RAH-66 Comanche

7 January 1994

Figure 3. HIDSS mass/center of mass chart, z-axis.
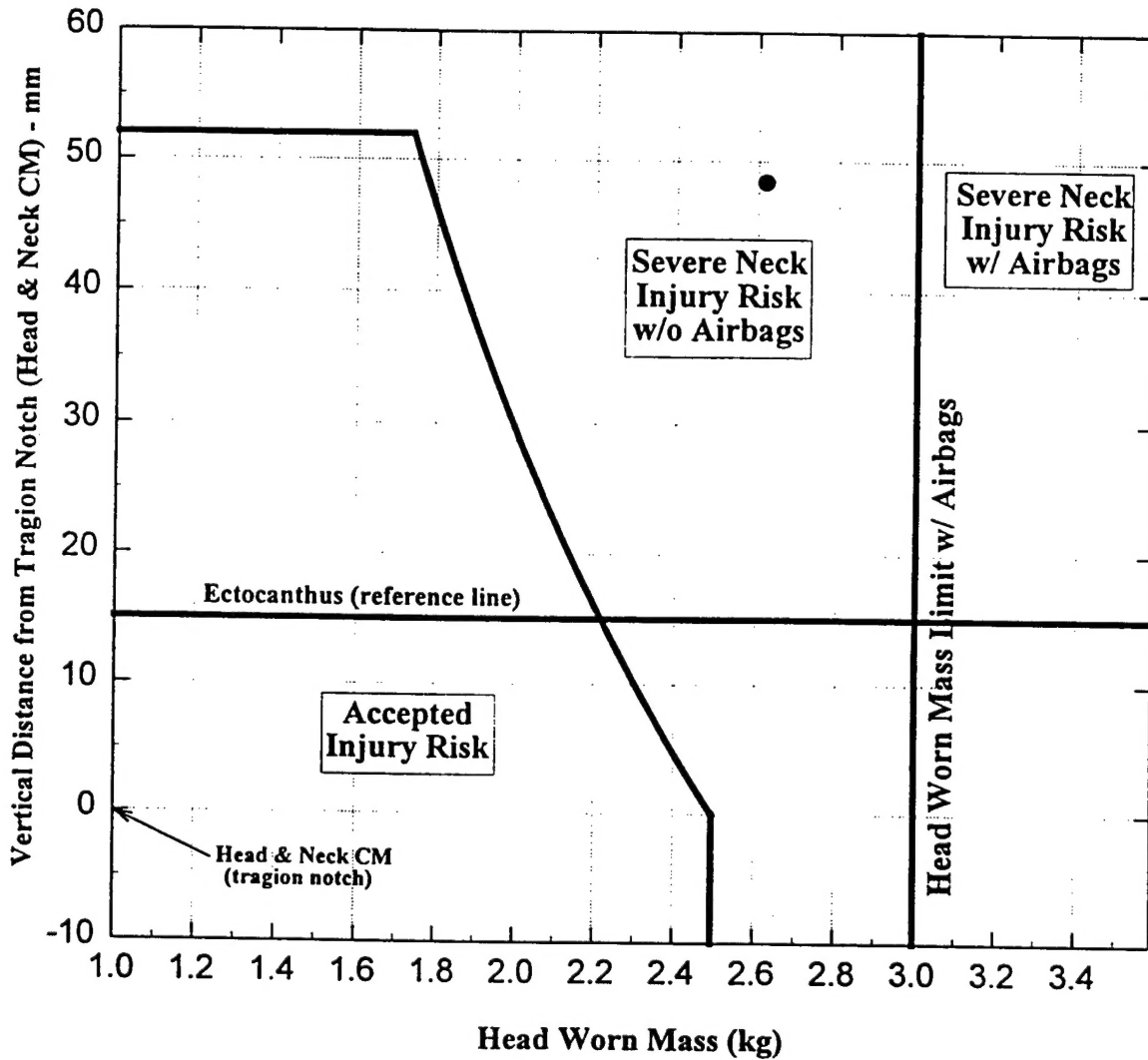
NOTES:

* Aviator fatigue and performance criteria are not considered.
* This figure supersedes all previous versions of USAARL's recommended head worn mass criteria.
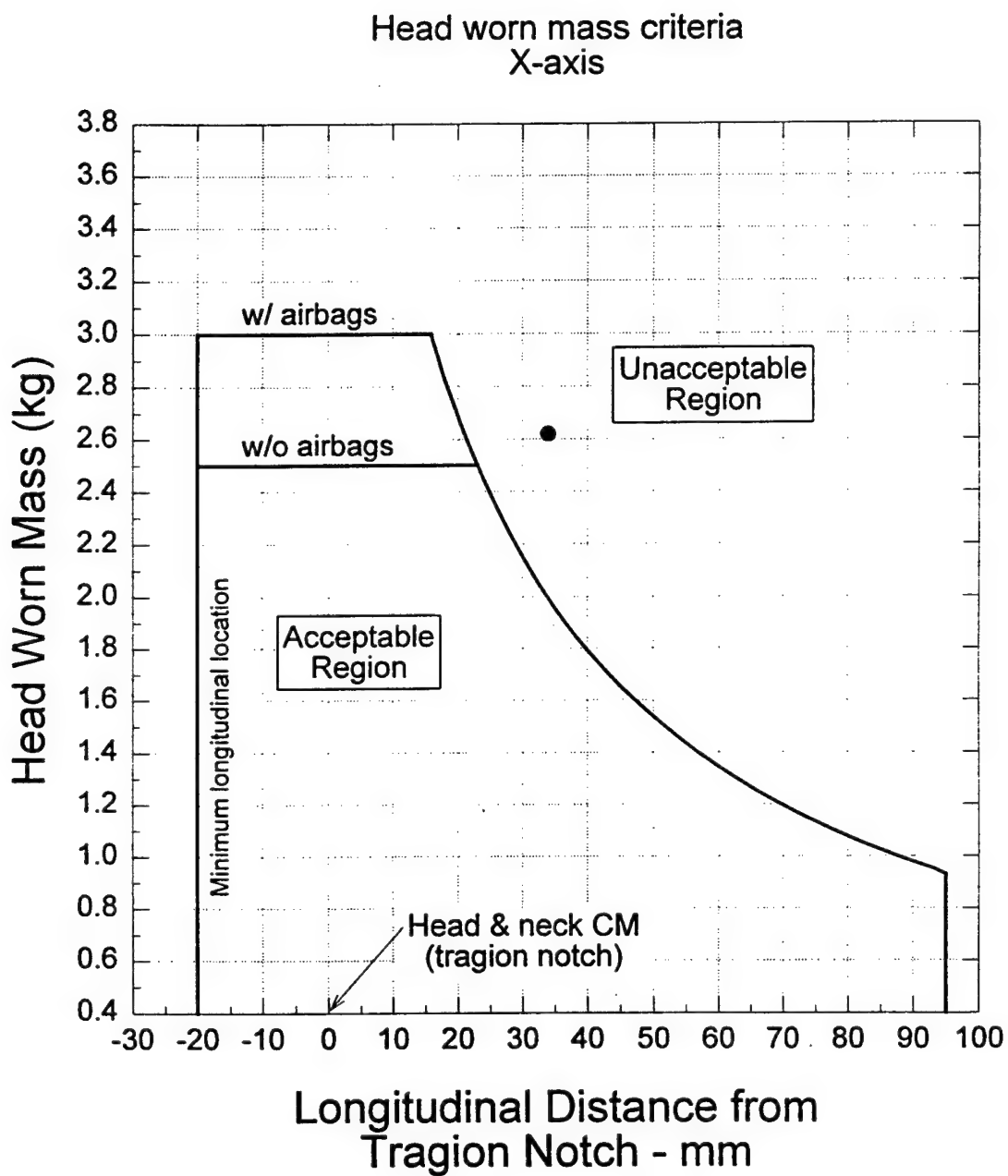
Figure 4. HIDSS mass/center of mass chart, x-axis.
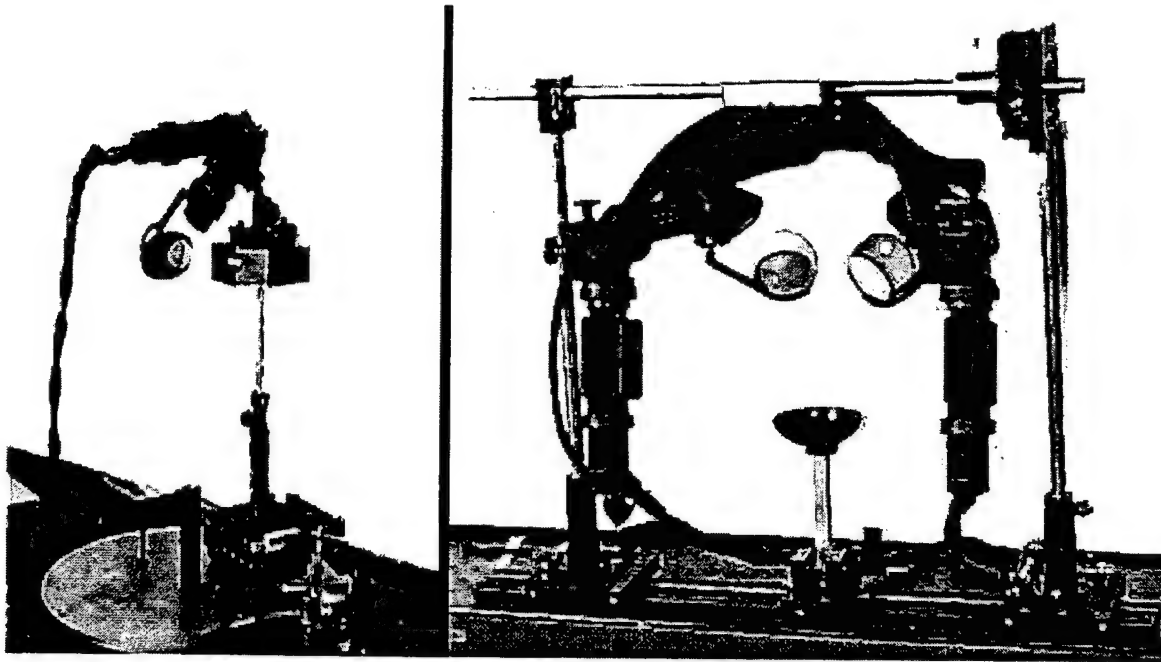
Figure 5. ARU mounting configurations.

FOV. Focusing our test equipment to infinity, we aligned our equipment with the video test target. We then focused on the exit pupil and aligned the test equipment with the middle of the exit pupil. Often, this process required several iterations to assure precise optical alignment. As per specifications, a video signal of 1023 scan lines with an aspect ratio of 6:5 was used.

Miniature CRT image source

Luminance output and response

Test equipment. Minolta Model LS110-1/3° luminance spotmeter, Tektronix 2440 digital oscilloscope, and a VII Pattern Master Model 2802 video generator.

Test procedure. The Minolta spotmeter was aligned with the center of the left channel CRT face. A full raster video test pattern was incremented in approximately 30-mv steps from 30 mv to 710 mv. Luminance readings were made at each luminance increment. Luminance amplitude was adjusted on the video generator to obtain the approximate incremental level as measured on the Tektronix oscilloscope. Both scene and contrast controls were set to maximum.

Results. The luminance response as shown in Figure 6 was monotonic and approached linearity, although a two component linear fit would probably provide a better description of the data. A linear regression analysis produced a slope of 4.87 with a Y-intercept of 24.61. The Pearson product moment correlation was greater than 0.98. Peak luminance was approximately 3300 fL.
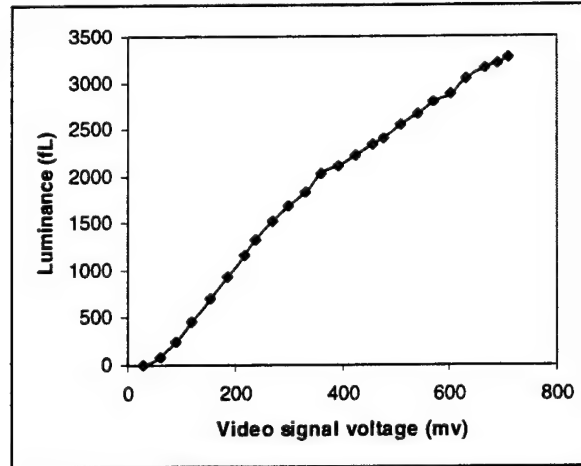
Figure 6. CRT luminance response.

Impact. The CRT provides a high luminance output (in excess of 3300 fL), which is required due to the inefficiency of the HIDSS's catadioptic design (see See-through spectral/luminance transmittance section below).

System

The following tests generally refer to the entire optical system including the CRT image source, relay optics, and combiner.

Field-of-view (FOV) (Physical measures)

Test equipment. Modified Oriel Model 13038 precision rotating stage with a large aluminum plate with additional weight support, Oriel Model number 18011 Encoder Mike Controller and custom computer software, Minolta Model number NT-1° luminance meter, and a dioptometer.

Test procedure. FOV was measured by rotating the left channel/CRT of the HIDSS about a point that was fixed at the center of the exit pupil. By ray tracing, it could be demonstrated that the image displayed by the channel was contained within a cone whose apex was at the exit pupil and extended out into space. By measuring luminance within this cone, we could measure the extent of the formed image. Following alignment, a uniform field was presented which covered the entire FOV. We measured the luminance of the horizontal FOV by rotating the stage through the spatial extent of the luminance cone. Following this measurement, we mounted the channel/CRT so that the vertical FOV could be measured. The procedure was repeated. Using a dioptometer with a crosshair, we measured the horizontal and vertical FOVs by measuring the total rotation required to transit the luminance profile.

Results. Figures 7a and b show the measured luminance profiles. The total FOV was found to be 36.7° (H) by 29.5° (V).

7
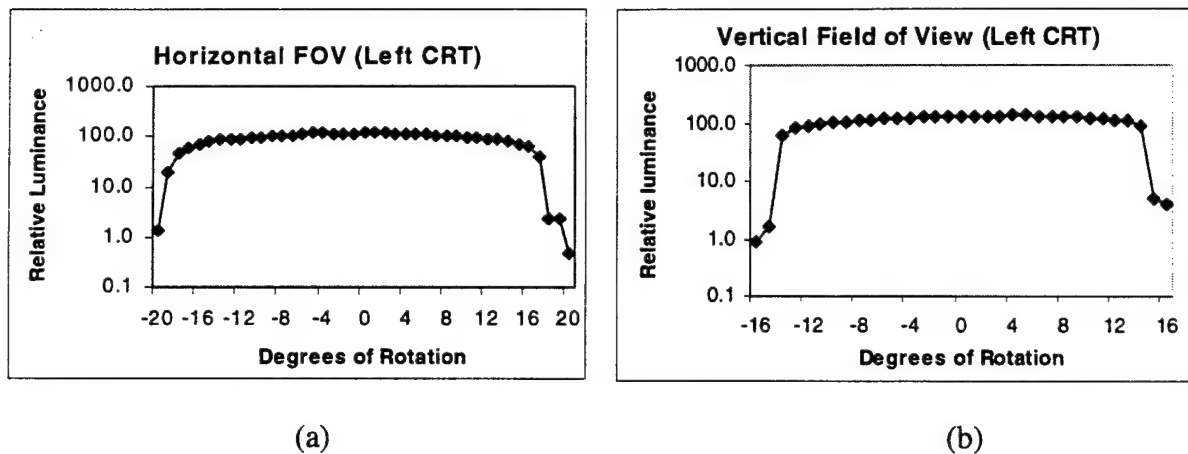
Figure 7. Luminance profiles for HIDSS horizontal (a) and vertical (b) FOVs.

Impact. The measured FOV is within tolerance for the HIDSS FOV goal.

Field-of-view (Perceptual measures)

Test equipment. Eye lane, target board, and a VII Pattern Master Model 2802 video generator.

Test procedure. The HIDSS ARU was mounted to an optical table so a chin rest could be mounted appropriately for viewing naturally through the combiner systems. A video pattern was generated in the HIDSS which clearly marked the center of the FOV while also showing the peripheral borders. An observer aligned the center of the FOV with a distant central fixation point on the fixed target board. We then marked on the board the left/right and top/bottom FOV borders for each eye.

Results. The monocular FOV measured 35.94° (H) by 29.72° (V). We measured a binocular FOV of 54.35° (H) by 29.7° (V).

Impact. The measured FOV is considered to meet the HIDSS binocular FOV design specification. Possible sources of deviation from the 52° specified value are IPD of observer, eye relief and subject error.

During this procedure, it was noticed that when the combiner is located at the design exit pupil position (22 mm behind the rubber baffles), it did not allow upward retraction of the combiner for this observer. This retraction is needed for monocular operation. However, when two observers tested at both the design eye position and the fore-aft position, which would allow combiner retraction, no notable reduction in FOV was found. However, based on our experience with head and facial anthropometry, a percentage of aviators will experience a reduction in FOV when the system is adjusted fore/aft to allow retraction of the combiners.

8

Image overlap

Test equipment. Eye lane, target board, and a VII Pattern Master Model 2802 video generator.

Test procedure. The HIDSS ARU was mounted to an optical table so a chin rest could be mounted appropriately for viewing naturally through the combiner systems. A video pattern was generated in the HIDSS which clearly marked the center of the FOV while also showing the peripheral borders. An observer aligned the center of the FOV with a distant central fixation point on the target board. We then marked on the board the right most edge of the left channel FOV and the left most edge of the right channel FOV. This procedure maps the binocular overlap region of the FOV.

Results. See Figure 8. The overlap region measured 17.53° horizontally.

Impact. The measured overlap is within approximately 0.5° of the 17° design specification.
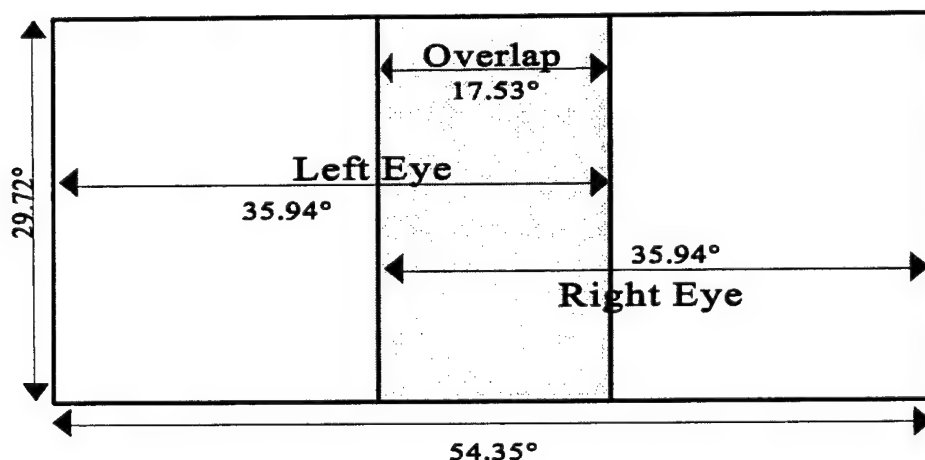
Figure 8. Monocular FOVs with overlap.

Visual field

Test equipment. Bausch and Lomb arch projection perimeter with a 3-mm spot size and 300-mm viewing distance, and a Haag-Streit projection perimeter with 1-mm spot size and 300-mm viewing distance, modified by replacing chin rest with forehead bar.

Test procedure. One observer was measured. Wearing the HIDSS with visor, the observer was aligned in the perimeter fixture. The visual fields were measured in 15-degree meridional intervals and plotted to show central obscurations for each eye. To control helmet and eye alignment, cross marks were placed on the visor face corresponding to the primary line of sight for each eye and separated by the observer's IPD. The alignment procedure was performed "by eye." The background illumination of the perimeter was adjusted to a minimal value such that

9

the observer could align the central visor marks with the center fixation point. A high contrast 1-mm target spot was moved in repeatedly from multiple meridians from the non-seeing region until detected. Because the PRU's size blocked some of the light from the targets at some peripheral angles, a second observer was used to verify the targets. For comparison, one observer's visual field for the upper and lateral parts of a medium-sized HGU-56/P with Aviator's Night Vision Imaging System (ANVIS) mount also were measured using a Bausch and Lomb perimeter. The line of sight points were marked at the IPD values at 1.5 inches below the styrofoam liner in accordance with Gentex Corporation fitting guidance. The spot size was 3 mm. The observer fixated on a central cross target on the perimeter screen. The targets were moved in repeatedly from multiple meridians from a non-seeing region until detected. The meridians were selected based on the irregular shape of the ANVIS mount. The data were plotted at 15-degree intervals.

Results. Figures 9-11 show the measured visual fields. Figure 9 shows the available binocular visual field when only the HIDSS PRU is being worn. Figures 10 and 11 show monocular visual fields for the left and right eyes when the ARU with baffles is attached.

Impact. The fields showing the obscurations due to the baffles are not absolute. The fields will change as a function of eye position. It was determined that the vertical limits of the HIDSS are similar to that measured for the HGU-56/P helmet. Look-under capability is judged better than what is available for ANVIS. Since visual fields were measured monocularly, and while binocular blind spots may exist, the plots seem to indicate the presence of only minimal binocular blind spots. The existence of blind spots, however, will likely be deemed an annoyance to aviators.

Interpupillary distance (IPD) and vertical adjustment

Test equipment. Exit pupil location device consisting of a section of rear screen projection material sandwiched between circular metal clamps, optical assembly with clamps and rod, and a millimeter rule.

Test procedure. Both optical channels were centered. The positions of the left and right exit pupils were found using the rear projection screen. The distance between the two positions was measured. The maximum IPD was measured as a function of vertical adjustment. To measure the vertical adjustment, a marker was placed on the combiner lens assembly which allowed measurement of the vertical extent with a millimeter rule.

Results. We measured a 68-mm IPD with the IPD adjustment knobs set to the middle mark ("0" mark). The IPD could be adjusted over a ±10 mm range (58 to 78 mm). The height adjustment had a ±5 mm range. With the optics raised to their highest extent, the IPD was reduced due to interference from the ARU. The largest available IPD was reduced by 8 mm to 70 mm. Figure 12 shows the plot of the maximum available IPD as a function of the vertical adjustment.

Visual Field Record
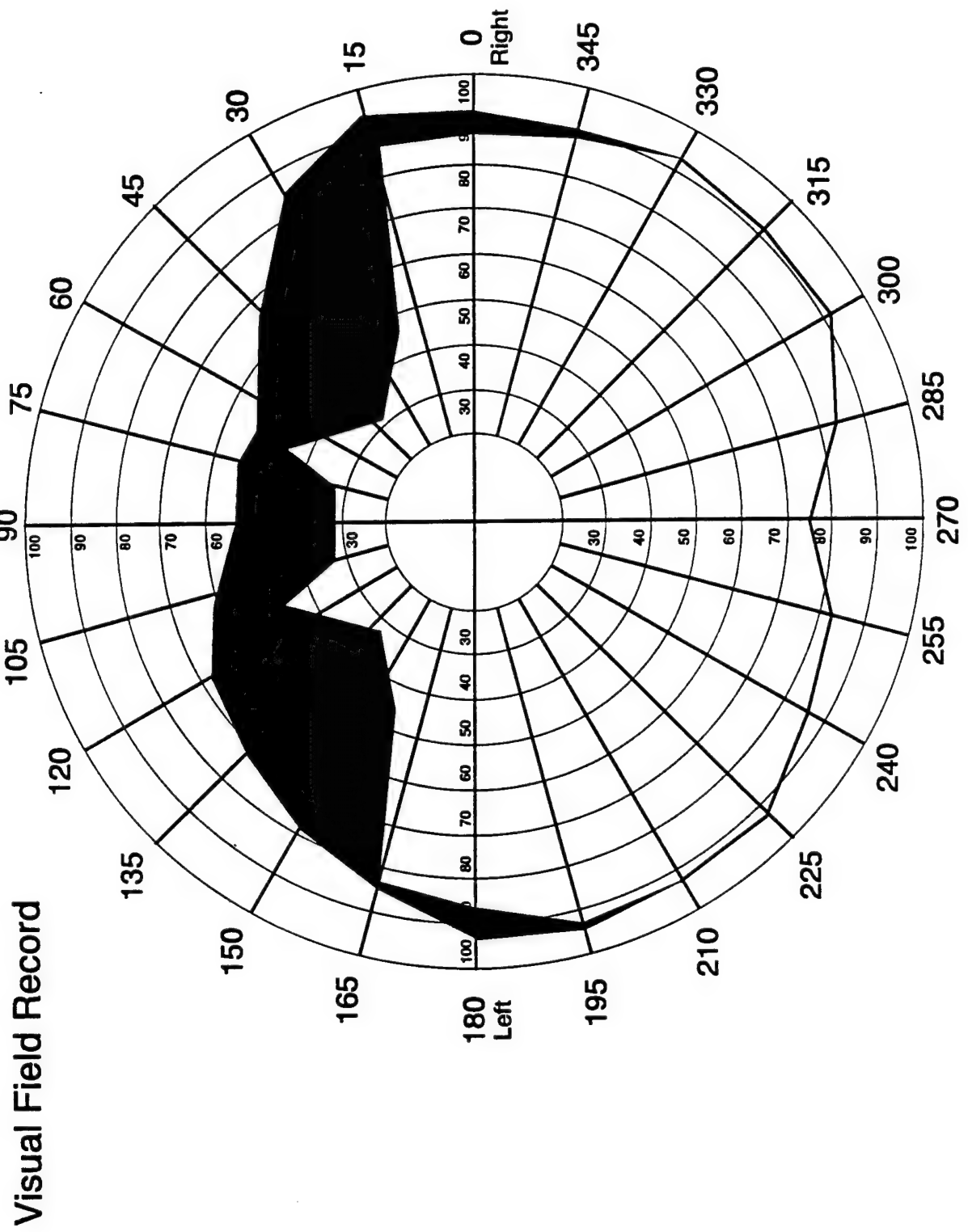
Figure 9. Binocular visual field for the PRU only.

Visual Field Record
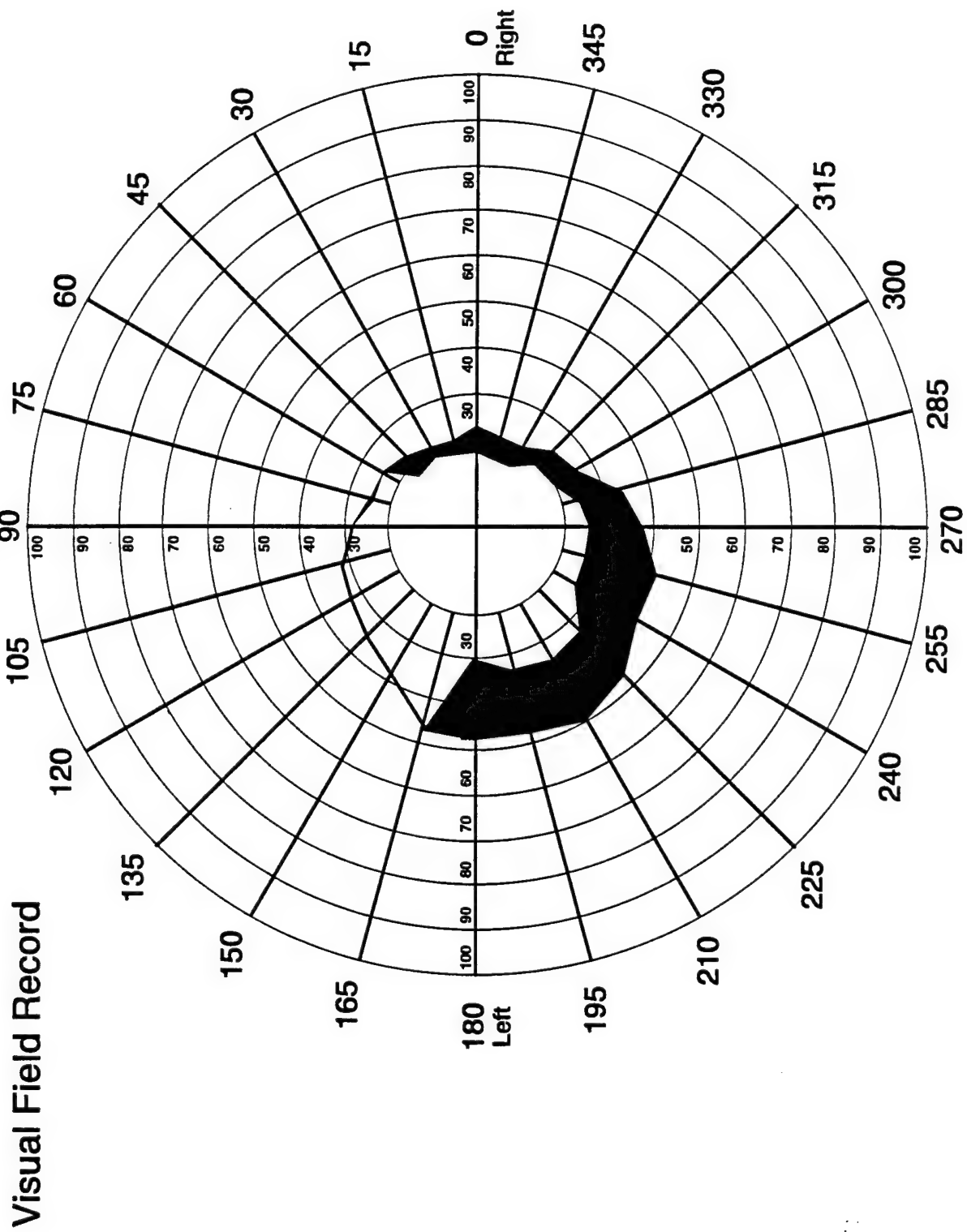
Figure 10. Monocular visual field for left eye with ARU and baffle.

12

Visual Field Record
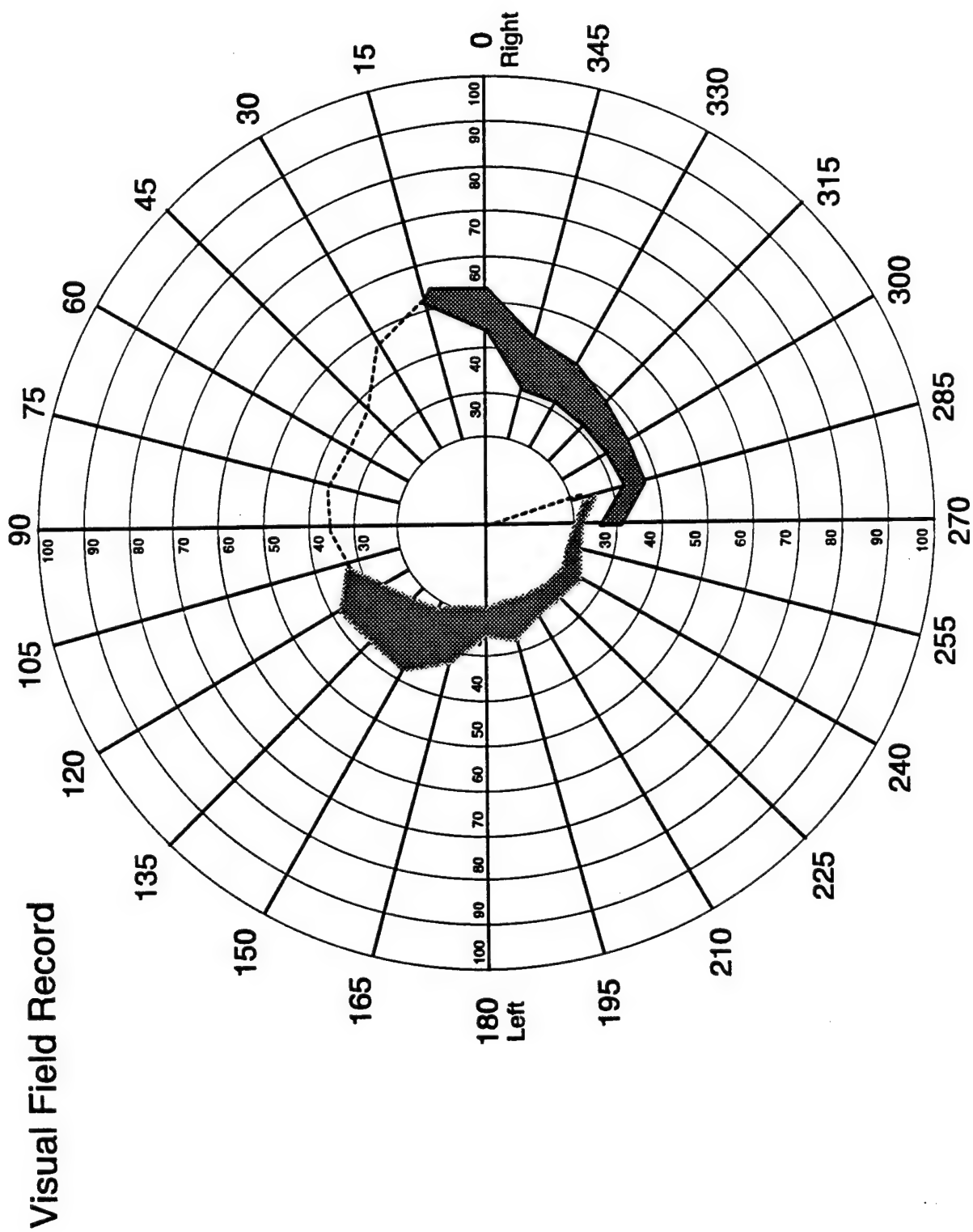
Figure 11. Monocular visual field for right eye with ARU and baffle. (Note: This visual field is slightly disjointed due to a shift in the helmet position during measurement.)
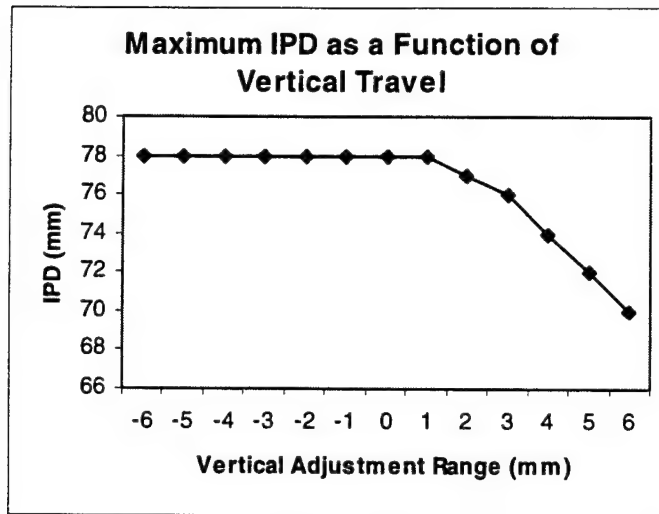
Figure 12. Maximum IPD as a function of vertical travel.

Impact. Head anthropometry affects fit. Fit affects the positioning of the eyes into the exit pupils and therefore FOV. Based on the measurements above and the aviator population, the effective IPD range is limited to a maximum of 70 mm. Based upon anthropometric data (Gordan et al., 1989), a 70-mm IPD corresponds to the 98th percentile female and 90th percentile male.

System transmittance and reflectance

Test equipment. Photo Research PR703A Spot SpectraScan and a Photo Research PR702A SpectraScan control console.

Test procedure. System transmittance was determined by measuring the luminance of the CRT at defined points within the optical path. A uniform field of maximum luminance was displayed on the CRT. First, the luminance of the CRT was measured. Second, the luminance from the CRT barrel was measured. Third, the luminance through the second lens (plano lens) was measured. Fourth, the luminance through the front lens (curved lens) was measured (Figure 13). Finally, the luminance was measured at the eye position by focusing on the exit pupil.

Results. The measured luminance values are given in Table 3. The overall system transmittance is 13.1%.

We place less value on these data than we do the see-through data below due to the difficulties in optical alignment and the confounding error that occurs through the measurement progression. Therefore, we estimate that the front lens (curved lens) has a nominal 20% transmittance with an 80% reflectance. For the plano lens, in which we have greater confidence, we estimate a 50/50 transmittance and reflectance ratio. Given the approximate 40% loss inside the barrel, we can estimate that only 12% of the light from the CRT reaches the eye (we measured 13.1%). Given

14

these nominal values, we can also estimate the see-through transmittance of the main peak of the P-53 phosphor. Given a nominal 20% and 50% transmittance for the two lens, we can estimate a see-through transmittance of only 10%. Compare this estimate to the spectral transmittance curves shown in Figure 14. We see an approximate 10% transmittance average for the wavelengths around 544 nm. We mathematically calculated the transmittance for the P-53 peak to be 11.2%. Based upon these data, we feel our nominal estimates of system characteristics are close.
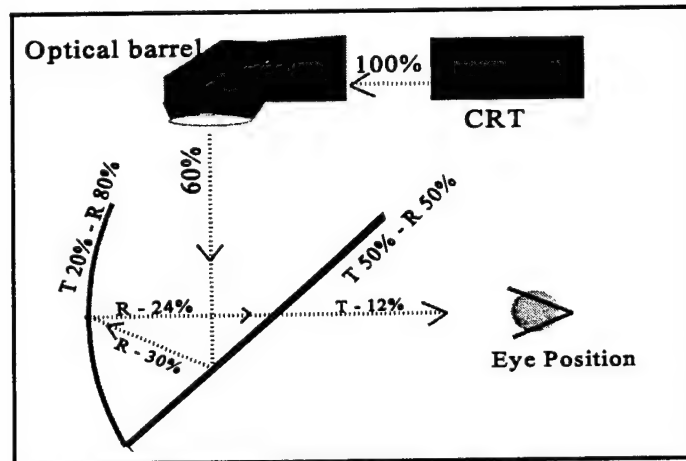
Figure 13. Luminance transmittance.

Table 3.
System luminance transmittance.

Position	Day luminance	Night luminance	Transmittance	Reflectance
1. CRT	3300 fL	425 fL		
2. CRT barrel	2000 fL	257 fL	60.6%	
3. Plano lens	1030 fL	133 fL	51.5%	48.5%
4. Front lens	121 fL	16 fL	11.7%	88.3%
5. Eye position	432 fL	56 fL		

Impact. With a 13.1% system transmittance, the catadioptic design is inefficient requiring high CRT luminance. However, the luminance at the eye seems sufficient for both night and daylight viewing.

15

Exit pupil size, position, and eye relief

Test equipment. Rear projection screen, dioptometer with crosshair reticle, Oriel precision positioners, and a millimeter ruler.

Test procedure. A rear projection screen was used to locate the exit pupil position. This was accomplished by moving the rear projection screen along the optical axis until a best focus was achieved. For determining exit pupil size, the dioptometer (with crosshair) was focused on the exit pupil. The crosshair was positioned at the extreme left edge of the exit pupil and the position was marked. The crosshair (dioptometer) was translated horizontally across the exit pupil to the extreme right edge of the exit pupil. The translational distance was recorded. The procedure was repeated for the vertical dimension. Eye relief (eye clearance distance) is defined for the purpose of this report to be the straight line distance from the cornea to the vertical plane defined by the first encountered physical structure of the system. For this test, eye relief was measured for two conditions: with and without the rubber baffles in place. Following the locating of the exit pupil, the distance back to the baffles was measured using a millimeter ruler. Three measurements were made and the average reported.

Results. Exit pupil was found to be located at a distance of 27.9 mm from the plane defined by the last (plano) combiner lens. Exit pupil shape was nearly circular with size measurements 15.1 mm vertically and 15.2 mm horizontally. With the rubber baffles attached (and needed to reduce extraneous reflections), the eye relief (eye clearance distance) was found to be 22.1 mm.

Impact. The design goal of a 15-mm exit pupil has been met. This goal was specified to reduce vignetting. The 27.9-mm eye relief value is not valid since this is based on not using the rubber baffles. The baffles are mandatory to reduce extraneous reflections. (See Extraneous reflections and Human factors issues questionnaire sections.) When the baffles are attached, eye relief is reduced to approximately 22 mm. The ability to use a chemical protective mask with this system should be considered marginal until evaluated.

See-through spectral/luminance transmittance

Test equipment. Oriel rotating stage, an RS-12 standard tungsten lamp, a Photo Research PR703A Spot SpectraScan and a Photo Research PR702A SpectraScan control console.

Test procedure. The RS-12 standard lamp was placed in front of the combiner lens assembly with the lamp surface orthogonal to the optical axis. The spectral output of the lamp was scanned with the combiner lens assembly in the retracted position ("up" position) and with the lens assembly in the normal (see-through) position. We also measured transmittance as a function of horizontal and vertical rotation to see if the optical coatings are angular dependent.

Results. The see-through spectral transmittance curves for a number of horizontal and vertical angular orientations are shown in Figure 14. Note the notch at 544 nm, the peak of the P53 CRT

16
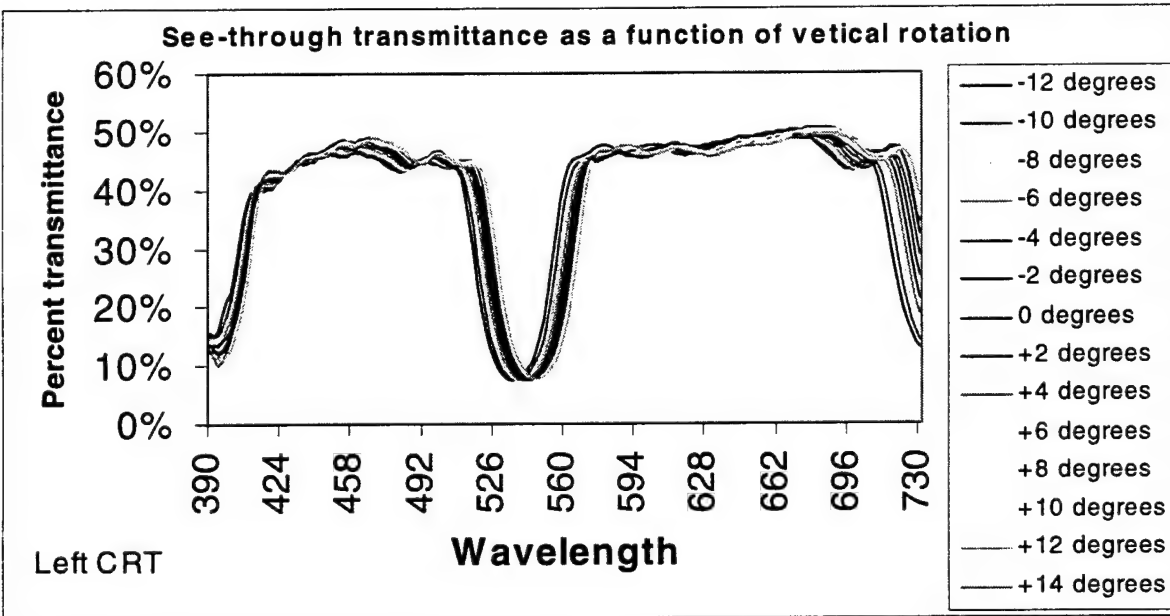
(a)
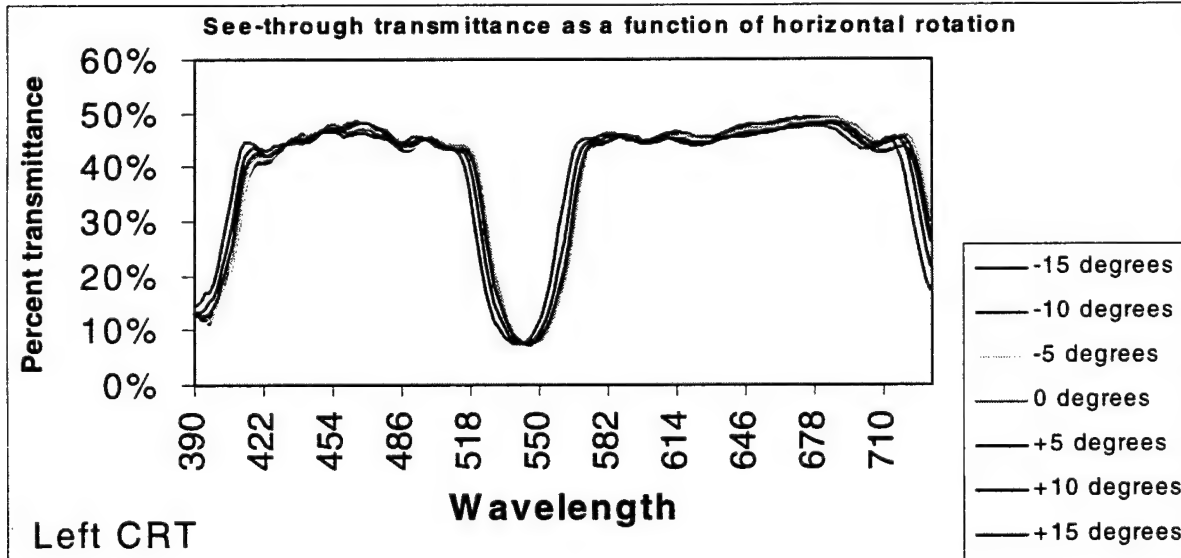
(b)

Figure 14. See-through spectral transmittance as a function of (a) horizontal and (b) vertical rotation.

17

image source phosphor. No significant angular effects were observed in the data. Transmittance on either side of the notch approaches 50%. Transmittance falls-off appreciably above 700 nm and below 420 nm. The average spectral transmittance across the measured spectral band (390 to 730 nm) is 40%. The see-through transmittance of a P53 phosphor display is estimated to be approximately 11%.

Impact. The combiners have a very small angular dependence and offer sufficient see-through capability. See Human factors questionnaire section.

Contrast ratio

Test equipment. VII Pattern Master Model 2802 video generator, Tektronix 2440 digital oscilloscope, and a Photo Research PR703A Spot SpectraScan.

Test procedure. The video generator and oscilloscope were used to produce bipartite boxes 20 mm square. Using a maximum output level of 710 mv, the total range was divided into 32 gray levels designated 0-31. Each square consisted of two gray level values. The background was set to the mid gray level value of 15. Luminance readings were measured for each side of the resulting square for 16 gray level pairs. The contrast ratio values were defined and calculated as $C_r = $ max/min. Contrast values were measured for both the "day" and "night" switch settings on the control panel.

Results. Contrast ratio measurements are provided in Tables 4 and 5. Plots are provided in Figures 15 and 16.

Square designation	Gray levels	Contrast ratio
1	14,16	1.1
2	13, 17	1.2
3	12, 18	1.3
4	11, 19	1.5
5	10, 20	1.6
6	9, 21	1.9
7	8, 22	2.3
8	7, 23	2.7
9	6, 24	3.3
10	5, 25	4.6
11	4, 26	6.4
12	3, 27	7.4
13	2, 28	13.4
14	1, 29	19.1
15	0, 30	21.5
16	0, 31	22

Table 4.
Contrast ratios, daytime.
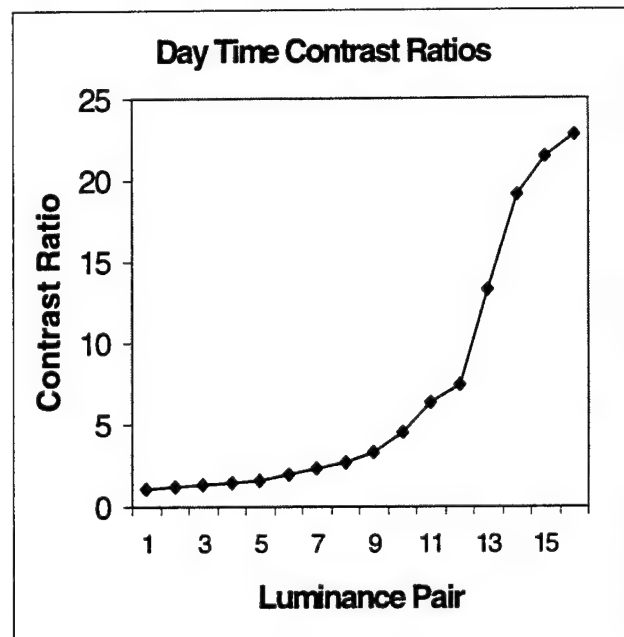
Figure 15. Contrast ratios, daytime.

Impact. By setting the background to a gray level of 15 (50 fL daytime and 1.4 fL night time), the resulting background had a decided effect upon the contrast ratios. The light from the background raised the light level of the dim half of the bipartite field, thereby lowering the contrast ratios. If we examine the line spread function data, we find that the peak of the luminance profile is approximately 400 times higher than the surrounding periphery (approximately 0.4 degrees from the illuminated line). The line spread data were collected under conditions where only the single line was illuminated. However, the contrast ratios were calculated based upon typical viewing conditions where small area contrast targets must be

Table 5.
Contrast ratios, nighttime.

Square designation	Gray levels	Contrast ratio
1	14,16	1.3
2	13, 17	1.8
3	12, 18	3.0
4	11, 19	4.9
5	10, 20	7.0
6	9, 21	13.1
7	8, 22	21.2
8	7, 23	25.6
9	6, 24	35.7
10	5, 25	36.7
11	4, 26	42.1
12	3, 27	49.3
13	2, 28	52.0
14	1, 29	52.7
15	0, 30	59.3
16	0, 31	66.0
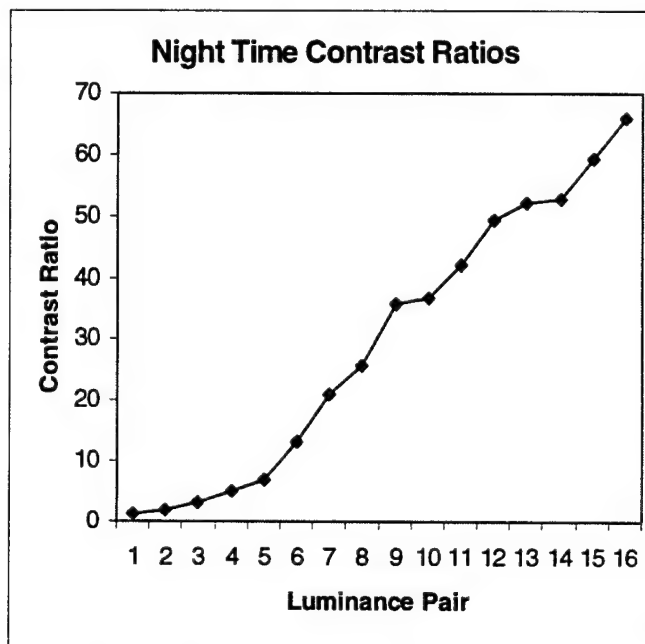
Figure 16. Contrast ratios, nighttime.

for nighttime conditions. The number of square-root-of-two shades of gray for the contrast ratio values of 22 and 66 are 9.9 and 13, respectively. This is verified when the available contrast ratio and shades of gray are theoretically calculated for the viewing conditions of 5000 fL ambient, 70% canopy transmittance, and 18% shaded visor transmittance and a CRT luminance of 3,300 fL. The resulting contrast ratio is 2.5 which correlates with 3.6 shades of gray.

Combiner power

Test equipment. Ann Arbor Optical tester with 50-line grating.

20

Test procedure. Power was determined by an increase in visible grating lines when the system under test was inserted into the optical path of the tester. Each additional line corresponded to a power of 0.037 diopter. A single measurement was made for each lens assembly.

Results. An increase in 5 lines was measured for each assembly, resulting in a power measurement of (5) x (0.037) = 0.185 diopter. A third lens assembly available from destructive testing was measured using the Humphry model 3222 lens analyzer and the measured power was 0.14 diopter.

Impact. These low values should not have any measurable impact on performance.

Luminance uniformity

Test equipment. Photo Research 1980 photometer and a VII Pattern Master 2802 video generator.

Test procedure. A uniform field luminance pattern was produced on the HIDSS left channel/CRT. At each of 25 positions corresponding to the intersections of the 10, 30, 50, 70, and 90% lines, the luminance was measured using the 1980 photometer with a 6' aperture.

Results. Figure 17 shows a luminance uniformity plot expressed in ±20% bands. The bands show deviation from the mean luminance. The maximum deviation from the mean was 69%. This occurred at the lower right corner of the image. The deviation for most of the image area was less than 40%. In the FOV periphery, significant luminance fall-offs were observed.

Impact. Current criteria (Rash, et al., 1996) states that the luminance at any two points within a flat field presented on a display should not vary by more than 20%. HIDSS specifications allow 20% variation based on the average luminance. By using the average luminance as our base measurement, we plotted the deviations from the mean. By this criteria, a significant central and peripheral region of the HIDSS FOV does not meet this criteria. The average deviation from the mean for the 25 samples was 21%. Based upon this analysis, we find that the HIDSS does not meet the specified criteria.

Field curvature and spherical/astigmatic aberrations

Test equipment. Dioptometer and a VII Pattern Master Model 2802 video generator.

Test procedure. A high definition grid pattern was produced on the full active area of the CRT. The optical/CRT channel was mounted on a rotating stage and positioned such that the center of rotation was at the exit pupil. The dioptometer was mounted to the optical table and aligned with the center of the test grid image. The position of the exit pupil was at the front of the dioptometer. The dioptometer was set to zero. From -18° to +18°, field curvature along the

Luminance Uniformity

10%

30%

50%

70%

90%

Vertical Position

10%   30%   50%   70%   90%

Horizontal Position

■ -100.00% to -60.00%   ■ -60.00% to -20.00%   ☐ -20.00% to +20.00%
☐ +20.00% to +60.00%   ■ +60.00% to +100.00%
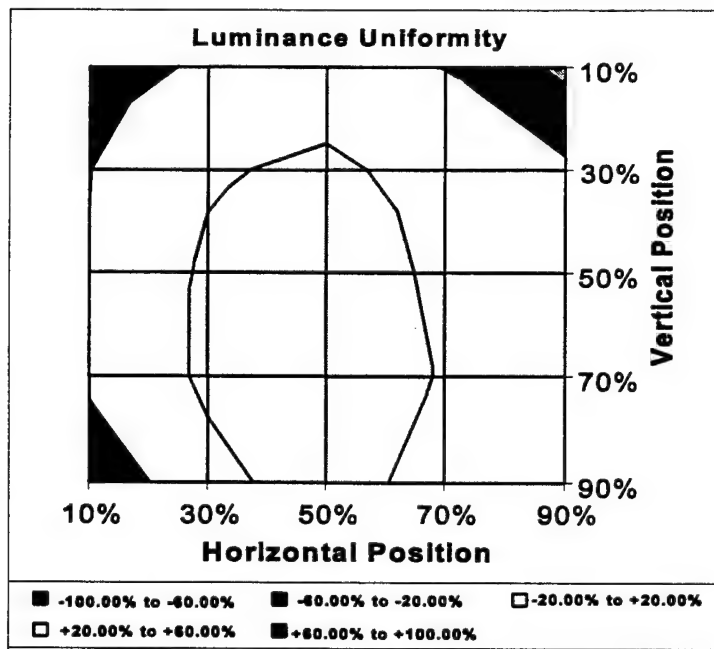
Figure 17. Plot of luminance uniformity with ± 20% bands.

horizontal axis was measured by focusing on the grid pattern and the power change noted. Astigmatic error was measured by noting any differences between vertical and horizontal grid focus.

By mounting the dioptometer to a precision traversing stage, spherical aberration could be measured as a function of decentration. Over a ±7 mm decentration range (the most allowed with a 15-mm exit pupil), spherical aberration was measured.

Results. No significant field curvature or spherical/astigmatic aberrations were measured: all measured values were less than 0.125 diopter.

Impact. The field curvature and optical aberrations were insignificant.

Temporal response (phosphor persistence)

Test equipment. Tektronix 2440 digital oscilloscope, VII Pattern Master Model 2802 video generator, and a Photo Research 1980 photometer.

Test procedure. A single horizontal scan line was displayed on the HIDSS left channel/CRT. A degree circular aperture was aligned on the middle of the horizontal line segment. We calculated that the CRT beam would be within the photometer's aperture for less than 1 μsec every 33.33 msec. This short measurement period allowed us to measure the phosphor rise and fall times.

22

Results. By defining the rise time to 90% of the peak, we found a phosphor rise time of approximately 500 μsec. By defining the phosphor fall time as the time from peak to 10%, we found a phosphor persistence of approximately 6 msec.

Impact. The measured 6 ms persistence is in line with the ~7 ms value cited in Tube Engineering Advisory Council (TEAC) publication No. 116. This is the limiting temporal characteristic of the HIDSS. The phosphor's temporal characteristics provide a sufficient temporal bandwidth for human perception.

Modulation transfer function (MTF)

Test equipment. Photo Research 1980 photometer with a slit aperture and 7-mm entrance pupil and a VII Pattern Master Model 2802 video generator.

Test procedure. The left channel/CRT was mounted on a rotating stage such that the axis of rotation coincided with the position of the exit pupil. A single vertical line segment was displayed in the middle of the FOV. The luminance of the line was adjusted to provide a high contrast ratio. The slit aperture in the 1980 photometer was aligned with the line segment. The slit aperture measured approximately 1 arc minute in width by 10 arc minutes in length. The slit was appreciably narrower than the video line segment. We rotated the table to a position 0.5 degrees laterally. The amount of rotation equivalent to 0.5 arc minutes was calculated. Photometric readings were taken at each 0.5 arc minute increment about the line segment. In all, 120 readings were obtained which encompassed 30 arc minutes to either side of the line segment. The resulting luminance profile was a line spread function of the single line segment. The fast Fourier transform (FFT) of the line spread was calculated and then normalized to approximate the uncorrected horizontal MTF. Likewise, the FFT of the finite slit aperture was calculated and normalized. The inverse of the aperture FFT was multiplied by the line spread FFT thus performing a deconvolution and correcting the effects of the finite aperture. The left channel/CRT then was rotated 90° to obtain the vertical line spread in similar fashion and the FFT procedures repeated.

Results. The normalized horizontal and vertical MTFs are shown in Figure 18. As expected, the vertical MTF is slightly higher than the horizontal MTF over spatial frequencies beyond 3 cycles/degree (c/deg). The MTFs have fallen to 50% at only 6 to 7 cycles per degree and are 90% down at only 10 to 11 cycles per degree.

Impact. The MTFs appear to be low given the spatial bandwidth of the visual system. We noticed that the lines appeared out of focus and this could account for part of the low spatial resolution.
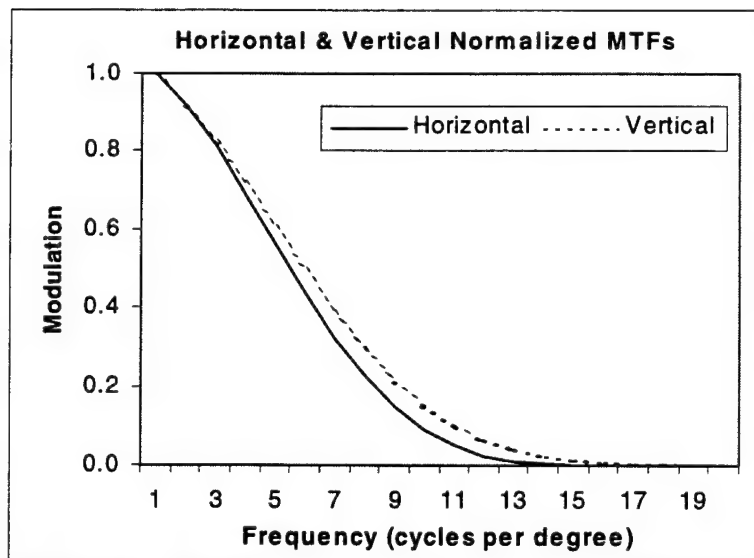
Figure 18. Normalized static MTFs for the horizontal and vertical meridians.

Luminance tracking

Test equipment. Photo Research 1980 photometer.

Test procedure. The ARU with left and right channels/CRTs was mounted to a lateral slide which allowed photometric measurements to be taken from each channel successively. The left and right channels were ganged such that right and left channel luminances advanced simultaneously. The channels were ganged by pushing the contrast inner knob inward.

Results. Luminance tracking results can be seen in Figure 19. As can be seen from the figure, the luminance tracking was highly linear.

Impact. A highly linear luminance tracking will allow aviators to adjust overall luminance without introducing left and right channel luminance disparity.

24

Luminance Tracking Between Channels
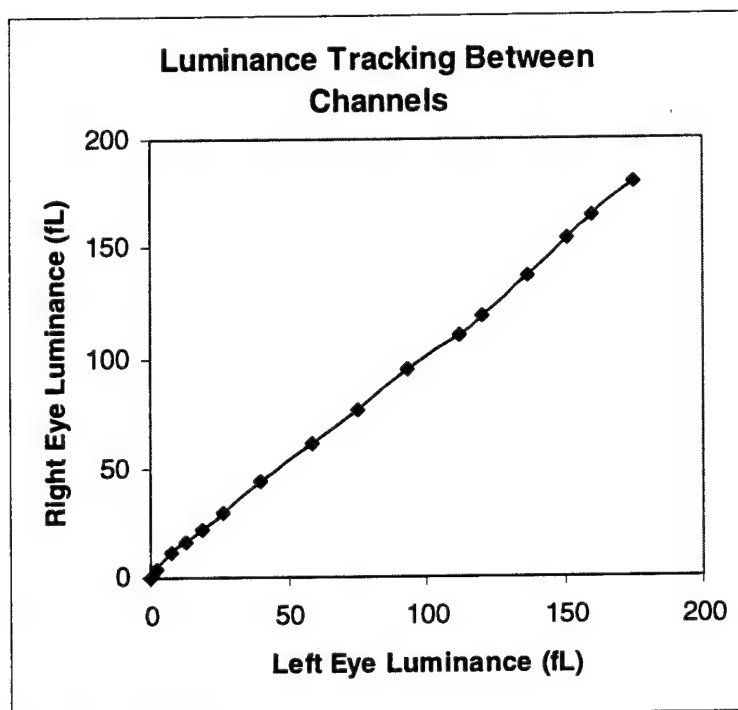
Figure 19. Left and right channel luminance tracking with ganged controls.

Visor performance

Visor measurements were performed at points 40 mm above the bottom line of the visor at an IPD of 64 mm centered about the visor center line.

Luminous transmittance

Test equipment. EG&G Gamma Scientific RS-12 reference lamp and a Minolta luminance spot meter, model 110.

Test procedure. Luminance measurements were taken of the reference lamp with and without the clear visor in the line of sight. Luminous transmittance was calculated from ratio of the "with" measurement to the "without" measurement and expressed as a percentage.

Results. Visor photopic transmittance was measured as 89%.

Impact. Visor transmittance meets the standard Army Class I visor requirement to have a transmittance of 85% or greater.

Refractive power

Test equipment. Allgeran Humphrey automatic lens analyzer, model 320.

Test procedure. The visor was set into lens analyzer in an "as worn" orientation. The lens analyzer reads spherical and cylindrical power and expresses them in units of 0.01 diopter.

Results.

Table 6.
Visor refractive power.

Left eye	Right eye
-0.05/0.00 diopter	-0.03/-0.05 diopter

Impact. Refractive power values are negligible and fall below the generally accepted "not to exceed" limits of ±0.125 diopter spherical and ±0.0625 diopter (MIL-V-43511C, 1990).

Prismatic deviation

Test equipment. Allgeran Humphrey automatic lens analyzer, model 320.

Test procedure. The visor was set into the lens analyzer in an "as worn" orientation. The lens analyzer reads spherical and cylindrical power and expresses them in units of 0.01 diopter.

Results.

Table 7.
Visor prismatic deviation.

	Left eye	Right eye
Vertical	0.01 BD	0.05 BD
Horizontal	0.20 BO	0.12 BO

Note: Values expressed in prism diopter; BD denotes base down; BO denotes base out.

Impact. According to MIL-V-43511C, measured values of prismatic deviation at both the left and right eye shall not exceed 0.18 diopter vertically and horizontally. One sample value (0.20 diopter BO) slightly exceeds this value. In addition, the algebraic difference between the eye points shall not exceed 0.18 diopter vertically and horizontally, and the algebraic sum shall not exceed 0.5 diopter horizontally. Table 8 presents these difference values for the sample.

Table 8.
Visor prismatic sum and differences.

Left eye	Right eye	Vertical difference	Horizontal difference	Horizontal sum
0.01 BD	0.05 BD	0.04		
0.20 BO	0.12 BO		0.08	0.32

Note: Values expressed in prism diopter; BD denotes base down; BO denotes base out.

All prismatic sums and differences meet the criteria. Caution must be exercised in making inferences regarding these conclusions since they are based on a single visor sample.

Distortion

Test equipment. Ann Arbor Optical tester with 50-line grating.

Test procedure. The visor sample was placed along the optical axis of the optical tester. The grating was viewed and the resulting image was compared subjectively to distortion standards provided in MIL-V-43511C.

Results. No detectable distortion was observed within the central vision area. Edge distortion was present but minimal.

Impact. The distortion levels present in the visor should not impact performance.

Visual performance

See-through Snellen visual acuity

Test equipment. American Optical Snellen acuity projection system.

Test procedure. Two observers wearing the HIDSS (i.e., looking through the combiner optics), but without a visor, were given a standard optometric visual acuity screening administered by a licenced optometrist. The Snellen characters were generated by an American Optical projection system.

Results. Both observers were measured to have 20/15 Snellen acuity with each eye.

Impact. See-through visual acuity with the HIDSS is not compromised.

27

See-through color discrimination

Test equipment. Dvorine Pseudo-Isochromatic plates and a Lanthony's desaturated D-15 hue test.

Test procedure. Two observers were tested using the Dvorine pseudo-isochromatic plate and the Lanthony desaturated D-15 hue tests. The Dvorine test consisted of 14 test plates viewed under a Macbeth easel lamp. The observer viewed plates and read the embedded numbers. No more than 5 seconds were allowed per plate. The Lanthony test consisted of 16 color chips (embedded in circular caps) selected from the Munsell Book of Color. The hues (Munsell hue) were selected so that the intervals between different hues were approximately equal. The mean chroma (Munsell chroma) was 2 and the mean luminosity level (Munsell value) was 8. The color caps had scoring values on the bottoms. A reference cap is fixed permanently to the left end of the lower panel of the rack. The remaining 15 caps are placed in random order on the upper panel of the rack. The subject's task was to arrange the color chip caps in order according to color. He was instructed to do this by first locating the color cap that most closely resembles the reference cap and placing it next to it, then selecting the color cap that most closely resembles the last selected cap, etc., until all of the caps were arranged in order. By closing the rack and turning it over, the scoring numbers became visible and the subject could be scored.

Results. Both observers correctly identified all 14 plates of the Dvorine Pseudo-Isochromatic plate test and identified all numbers in the Lanthony desaturated D-15 hue test.

Impact. The ability to read and interpret color information within the cockpit is not compromised when wearing the HIDSS.

Pedestrian characteristics

Extraneous reflections

Test equipment. Sun and Lockheed-Martin Comanche simulator, Fort Rucker, Alabama.

Test procedure. The presence and perceived intensities of extraneous reflections were evaluated for two viewing conditions: Outside in direct sunlight (solar altitude, 45°; sky, clear; illumination, 71,000 lux (6,600 fc); HIDSS: Day mode, full brightness and contrast; visor, clear and tinted; temperature, 83.5°F in sun, 78.3°F in shade) and in the Lockheed-Martin Comanche simulator with full cockpit and instrumentation lighting. For the outside, daytime evaluation, two observers donned the PRU/ARU and moved their heads through a full range of motion for the purpose of detecting extraneous reflections. For the Lockheed-Martin Comanche simulator evaluation, four observers moved their heads through a full range of motion for the purpose of detecting extraneous reflections. In the simulator, reflections were assessed both with and without the rubber baffles. (See human factors issues questionnaire section.)

Results. Daytime, outside - When wearing a clear visor and oriented about 45° to either side of a direct line of sight to the sun with the head tilted up approximately 15°, an intense narrow, elongated sun reflection was visible over a 5° range. The reflection is best described as two closely spaced vertical bands. When the tinted visor was used, the reflections were reduced in intensity but retained the same contrast, implying the source of the reflections is the optics.

Comanche simulator - Without the baffles installed, all observers reported the reflections to be "overwhelming" and "unacceptable." With the baffles, observers could still pick up the reflections off the windows. But, these were judged to be only "slightly annoying" and could be "lived with." It is not known whether or not the simulator windows model the Comanche canopy.

While performing the daytime, outside evaluation, it was noticed that when observed from the exterior at a specific angle, a highly intense sun glint results.

Impact. Reflections are going to be a problem. The rubber baffles do dislodge rather easily and are not easily replaced. The design of the baffles should be further investigated. At night without the baffles, extraneous reflections, which will be present, are unacceptable.

Daylight performance

Test equipment. Sun.

Test procedure. Two observers were asked to evaluate the ability to see imagery operating in day mode under the following conditions - Outside in direct sunlight (solar altitude, 45°; sky, clear; illumination, 71,000 lux (6,600 fc); HIDSS: Day mode, full brightness and contrast; and visor, tinted).

Results. Both observers reported that imagery was viewable against all backgrounds except directly into the sun.

Impact. Except for viewing against the sun (unfeasible) and against white clouds (not tested), the imagery (symbology not available) was viewable. However, the number of perceptible shades of gray was not determined.

Human factors issues questionnaire

Test equipment. Link-Martin Comanche simulator, Fort Rucker, Alabama.

Test procedure. Four observers (3 Comanche simulator pilots and 1 vision scientist) were asked to respond to questions addressing numerous human factors issues associated with the HIDSS. Two of the observers wore corrective lenses.

Results.

1. <u>Assess ease of donning and doffing PRU (helmet) only</u>: Three observers rated the ease of donning and doffing as "very easy." One of the observers would require a larger sized helmet. (The helmet provided was size "large.") This resulted in the observer's eyes being located closer than desired for alignment of the HIDSS eyepieces.

2. <u>Assess the ease of attaching and detaching the ARU (HMD)</u>: Observers required about four trials to become accustomed to attaching the ARU. After this period, all observers rated the ease of attaching and detaching of the ARU as "easy." All of the Comanche simulator pilots stated that the ARU under evaluation was easier to attach than the one currently in use in the simulator.

3. <u>When within exit pupil, can the combiners be pushed up to allow monocular operation?</u> With a fore-aft setting to the line marked on the helmet mount, none of the observers could retract either of the combiners.

4. <u>Assess lowering and raising of the visor</u>: Lowering the visor was noted as being easier and preferred over the one currently used. However, most observers commented that they probably would not lock the visor down (at least not both sides).

5. <u>Assess ease of using IPD adjustment</u>: All observers rated the IPD adjustment as "excellent."

6. <u>Assess ease of using vertical adjustment</u>: All observers rated the vertical adjustment as "excellent."

7. <u>With cockpit instrumentation and lighting on, describe presence and brightness of extraneous reflections</u>: Reflections were assessed both with and without the rubber baffles. Without the baffles installed, all observers reported the reflections to be "overwhelming" and "unacceptable." With the baffles, observers could still pick up the reflections off the windows. But, these were judged to be only "slightly annoying" and could be "lived with."

8. <u>Assess look under/around viewing</u>: Observers judged look under/around viewing to be "as good as with ANVIS."

9. <u>With cockpit instrumentation on, assess look-through vision</u>: Observers judged look-through vision as "excellent" for the cockpit displays including the electroluminescent panels. All observers noticed a slight "pinkish" tint, but all colors could be distinguished. However, the buttons on the panel mounted displays were less viewable through the combiners due to the low illumination levels in the cockpit. It should be noted that looking through the combiner is not anticipated to be a routine action. The combiner would normally be retracted.

10. <u>Were any physical compatibility problems encountered?</u> Observers encountered head motion restriction when wearing the HIDSS. This restriction came in the form of the lower portion of the CRT barrel striking the shoulders. Observers also expressed concern with the

30

possibility of increased problems when wearing the 50-cal chicken plate and shoulder harness (not present in the simulator).

11. Additional comments: Two observers mentioned the forward CM shift, but liked the low weight. These individuals said they "would use a small counterweight" to move the CM back and reduce "hot spots" and helmet rotation. The two observers who wore glasses experienced no compatibility problems. Overall, all of the observers liked the HIDSS.

Impact. The HIDSS seemed to be well received. However, the forward CM is a problem for which the addition of a counterweight will be the unofficial solution. Unfortunately, this additional weight will exacerbate the already identified safety issue of head supported weight. The motion restriction problems, real and anticipated, where the bottom CRT barrel strikes the shoulders and other aviator mounted systems, is an important issue which must be resolved.

Single visor configuration

The DVP HIDSS has a single visor configuration. A recent study of visor use among U.S. Army aviators shows that single visor configurations reduce visor usage (Rash et al., 1997). This reduced usage can be correlated to an increase in frequency and severity of facial injuries (Reynolds et al., 1997). Such injuries can incur significant dollar costs due to equipment loss, loss of service, and benefits for injury or death (Zilioli, 1971; Zilioli and Bisgard, 1971). The Army's last two fielded helmets, the SPH-4B and HGU-56/P, both have dual visor configurations.

Summary and discussion

Evaluation results are summarized in Table 9. The critical areas of HIDSS performance are head supported weight (mass), CM, and image quality. Measurements show that the HIDSS fails to provide acceptable weight and CM performance. At a value of 2.62 kg, head supported weight exceeds the maximum allowable value. In addition, the HIDSS was determined to exhibit a significant forward shift in CM which, based on experience, would result in aviators adding counterweights, further increasing weight. The measured HIDSS values fall outside of the USAARL established weight/CM crash injury curves. Interpretation of this failure indicates that RAH-66 Comanche aircrew will be exposed to a greater risk of head/neck injury during mishaps than other Army aircrew.

Image quality consists of a number of attributes which address spatial, temporal, luminance, and spectral figures-of-merit. The HIDSS provided acceptable image quality except for the areas of contrast ratio (shades of gray), luminance uniformity, and MTF. During daytime operation (5000 fL typical), the HIDSS does meet the required 3.0 shades of gray. However, if HIDSS imagery is intended for day pilotage usage, the measured gray shades appear insufficient. For luminance uniformity, a significant drop-off was exhibited in the peripheral FOV. The CRT

Table 9.
Evaluation summary.

System	Parameter	Measurement Data	Page
Biodynamics	Center of mass	x-axis: 34.02 mm; y-axis: 3.38 mm; z-axis 48.41 mm.	2
	Mass	Total HIDSS head supported weight (mass) of 2.62 kg.	2
Optics	CRT luminance response	Quasi-linear response with a high of 3300 fL	6
	Field of view (physical)	Each Optical Channel: Horizontal FOV = 36.7°; Vertical FOV = 29.5°	7
	Field of view (perceptual)	Binocular FOV = 54.35° by 29.7°	8
	Image overlap	Binocular Overlap = 17.53° with flanking monocular fields of 18.41°	9
	Visual field	Obscurations due to baffles; improved look under capability over ANVIS.	9
	Interpupillary distance and vertical adjustment	58 to 78 mm IPD range for most optical positions with a 10 mm vertical adjustment range. With the optics raised to their highest extent, the maximum IPD is reduced to 70 mm.	10
	System transmittance & reflectance	From HIDSS CRT to Eye: P-53 phosphor luminance is reduced by 87%.	14
	Exit pupil size, position and eye relief	Size: The exit pupil is circular in shape with diameter of 15.15 mm. Position: 27.9 mm behind the plano lens. Eye Relief: 22.1 mm behind the baffle.	16
	See-through spectral luminance transmittance	The average spectral transmittance is about 40% although the transmittance function has a large trough near the peak of the P-53 phosphor. The see-through transmittance of the peak of the P-53 phosphor is about 11%.	16
	Contrast ratio	Day time setting: $\approx$ 22; Night time setting: $\approx$ 66	18
	Combiner power	0.185 diopter.	20
	Luminance uniformity	Significant drop-off in the periphery. Luminance uniformity was not within the specified ±20% deviation from the average luminance.	21
	Field curvature & spherical/astigmatic aberrations	No significant effects.	21
	Temporal response	Phosphor: rise time of 500 μsec; fall time of 6 msec.	22
	MTF	Normalized MTF down by 50% at 6 to 7 cycles/degree.	23
	Luminance tracking	Quasi-linear tracking response.	24

Table 9 (cont.)
Evaluation summary.

System	Parameter	Measurement Data	Page
Visor	Luminous transmittance	Photopic transmittance measured at 90.2%	25
	Refractive power	Negligible: -0.05 diopter or less.	26
	Prismatic deviation	No significant effects.	26
	Distortion	No detectable distortion.	27
Visual performance	See through visual acuity	20/15 Snellen acuity in each eye.	27
	See through color discrimination	No color discrimination defects detected.	28
Pedestrian characteristics	Extraneous reflections	Extraneous reflections were present even with the baffles in place.	28
	Daylight performance	Imagery viewable but perceptible shades of gray not characterized..	29
	Human factors	Easily donned and doffed; ARU easily attached/detached; lowering/raising of visor acceptable; ease of use of IPD and vertical adjustments rated excellent.	29
	Single visor configuration	Results in lower usage of visor which increases frequency and severity of facial injuries during mishaps.	31

electron beam appeared out of focus and this contributed to the poor MTF response, down by 50% at only 6-7 cycles/degree.

Additional human factors engineering concerns surfaced during the evaluation. These included restrictions on pilot head movements due to CRT size and location, extraneous reflections, single visor configuration, and IPD extreme adjustment effect on monocular operation.

Conclusions and recommendations

The failure of the HIDSS to meet the USAARL weight and CM criteria will result in greater risk of head/neck injury during mishaps to RAH-66 Comanche aircrew. The HIDSS image quality was generally found to be acceptable except for the areas of daytime contrast ratio, luminance uniformity, and MTF. The measured contrast ratios (shades of gray) are considered insufficient for day pilotage usage (however, the requirement for the use of daytime pilotage FLIR has not been determined). For nighttime operations, there is a sufficient contrast ratio. While the luminance uniformity of the HIDSS showed a significant drop-off in the peripheral FOV, insufficient data exist to conclude actual pilot performance effects. The relatively poor MTF response was somewhat caused by an apparent out-of-focus electron beam. Also, of

considerable concern, are the issues of extraneous reflections, lack of dual visor configuration, and the lack of an optical focus adjustment.

The Development and Validation CRT based version of the HIDSS evaluated herein should be considered unacceptable in its present configuration. This conclusion is based primarily on system packaging which has resulted in an unacceptable weight and CM. For image quality, the issue of the poor MTF needs to be investigated

References

Department of Defense. 1990. Military specification: Visors, flyer's helmet, polycarbonate, MIL-V-43511C, dated 16 July 1990. Washington, DC.

Gordon, C . C., Churchill, T., Clauser, C. E., Bradtmillwe, B., McConville, J. T., Tebbetts, I., and Walker, R. A. 1989. 1988 anthropometric survey of U.S. Army personnel: Methods and summary statistics. Natick, MA: U.S. Army Natick Research, Development and Engineering Center. Technical Report Natick/TR-89/004.

McEntire, B. J., and Shanahan, D. F. 1996. Mass requirements for helicopter aircrew helmets. Presented to the AGARD Conference on Impact Injury Responses, Mechanisms, Tolerance, Treatment, and Countermeasures, 1996 November, Alamagordo, NM.

Rash, C. E., Mora, J. C., Ledford, M. H., Reynolds, B. S., Ivey, R. H., and McGowan, E. 1997. Visor use among U.S. Army rotary-wing aviators. Fort Rucker, AL: U.S. Army Aeromedical Research Laboratory. USAARL Report No. 98-16.

Rash, C. E., Mozo, B. T., McLean, W. E., McEntire, B. J., Haley, J. L., Licina, J. R., and Richardson, L. W. 1996. Assessment methodology for integrated helmet and display systems in rotary-wing aircraft. Fort Rucker, AL: U.S. Army Aeromedical Research Laboratory. USAARL Report No. 96-1.

Reynolds, B. S., Rash, C. E., Ledford, M. H., Mora, J. C., Colthirst, P. M., and Ivey, R. H. 1997. The role of protective visors in injury prevention during U.S. Army rotary-wing aviation accidents. Fort Rucker, AL: U.S. Army Aeromedical Research Laboratory. USAARL Report No. 98-18.

Tube Engineering Advisory Council. 1980. Optical characteristics of cathode ray tube screens. Washington, DC: Electronic Industries Association. TEPAC Publication No. 116.

Zilioli, A. E. 1971. Crash injury economics the cost of running and maintaining an Army aviator. Fort Rucker, AL: U.S. Army Aeromedical Research Laboratory. USAARL Report No. 71-17.

Zilioli, A. E., and Bisgard, J. C. 1971. Crash injury economics. Injury and death costs in Army UH-1 accidents in fiscal year 1969. Fort Rucker, AL: U.S. Army Aeromedical Research Laboratory. USAARL Report No. 71-18.

Appendix.

List of manufacturers.

Allergan Humphrey
3081 Teagarden Street
San Leandre, CA 94577

American Optical Corporation
Buffalo, NY 14215

Ann Arbor Testing Laboratories, Inc.
Ann Arbor, MI 48106

EG&G Gamma Scientific, Inc.
3777 Ruffin Road
San Diego, CA 92123

Gentex Corporation
Carbondale, PA 18409

Kaiser Electronics
2701 Orchard Parkway
San Jose, CA 95131

Minolta Camera Company Ltd
101 Williams Drive
Romsey, NJ 07446

Oriel Corporation
250 Long Beach Blvd
P.O. Box 872
Stratford, CT 06497

Photo Research
3000 North Hollywood Way
Burbank, CA 91505

Tektronix
P.O. Box 1520
Pittsfield, MA 01202-9864
http://www.tek.com